Sensitivity of a numerical wave model on wind re-analysis datasets

Citation for published version:
Lavidas, G, Venugopal, V & Friedrich, D 2017, 'Sensitivity of a numerical wave model on wind re-analysis datasets', *Dynamics of Atmospheres and Oceans*, vol. 77, pp. 1. https://doi.org/10.1016/j.dynatmoce.2016.10.007

Digital Object Identifier (DOI):
10.1016/j.dynatmoce.2016.10.007

Published In:
Dynamics of Atmospheres and Oceans

Sensitivity of a Numerical Wave Model on Wind Re-Analysis Datasets

George Lavidas[a,*], Vengatesan Venugopal[a], Daniel Friedrich[a]

[a] *Institute for Energy Systems, The University of Edinburgh, The King's Buildings, Mayfield Road, Edinburgh EH9 3JL*

Abstract

Wind is the dominant process for wave generation. Detailed evaluation of metocean conditions, strengthen our understanding of issues concerning potential offshore applications. However, the scarcity of buoys and high cost of monitoring systems pose a barrier to properly defining offshore conditions. Through use of numerical wave models, metocean conditions can be hindcasted and forecasted providing reliable characterisations.

This study reports the sensitivity of wind inputs on a numerical wave model for the Scottish region. Two re-analysis wind datasets with different spatio-temporal characteristics are used, the ERA-Interim Re-Analysis and the CFSR-NCEP Re-Analysis dataset. Different wind products alter results, affecting the accuracy obtained. The scope of this study is to assess different available wind databases and provide information concerning the most appropriate wind dataset for the specific region, based on temporal, spatial and geographic terms for wave modelling and offshore applications. Both wind inputs resulted results from the numerical wave model with good correlation. Wave results by the 1-hour dataset have higher peaks and lower biases, in expense of a high scatter index. On the other hands, the 6-hour dataset has lower scatter but higher biases. The study, shows that how wind dataset affect the numerical wave modelling performance and that depending on location and study needs, different wind inputs should be considered.

Keywords: Wave modelling, SWAN, Wind Re-Analysis

*Corresponding author

Email address: G.Lavidas@ed.ac.uk (George Lavidas)

1. Introduction

Waves and offshore environments have been a part of research for decades, however when considering energy production by renewable energy (RE) systems, understanding and evaluating the available resource is of major importance. Continuous research developments have provided tools that allow us to simulate, hindcast, and forecast sea states, through use of numerical modelling. Currently, we are in the third generation of numerical wave models, that are applied to oceanic and nearshore (coastal) applications (Komen et al., 1994; Holthuijsen, 2007).

One of the most important aspects in the use of numerical wave models is the quality of inputs, for both oceanic or coastal applications. Wind is one of the key parameters for wave generation and propagation. Wind data are provided by various international and local governmental bodies. Each organisation uses different Re-analysis techniques and usually based on different atmospheric models, providing datasets with various temporal and spatial resolutions. In this study two of the most recent products of such models are used, the ERA-Interim Re-Analysis from European Centre for Medium-Range Weather Forecasts (ECMWF) (Dee et al., 2011), and CFSR-NCEP Re-Analysis dataset provided by the National Centre for Atmospheric Research and the National Oceanic and Atmospheric Administration (NOAA), (Saha et al., 2010). They are used to compare the performance of hindcast by a nearhore wave numerical model applied in Scotland, previously taglobal inter-comparison study between has been outlined by Stopa and Cheung (2014) emphasising the differences of wind datasets.

Variability of data and lack of recording wind stations in offshore environments, drove researchers to investigate the validity and accuracy levels of the predicted wind by coupling them with large oceanic numerical models (Bidlot et al., 2005, 2006). Previous studies assessed the data information of several re-analysis datasets using existing wind measurements (Caires et al., 2004; Stopa and Cheung, 2014), buoy and numerical models were used to establish the optimal wind dataset. Results however were mixed, indicating different correlations between wind and waves depending on location, for the Northern or South Hemisphere (Stopa et al., 2013).

Due to the extent of the wind resource examination, previous studies used oceanic models to investigate and assess the wind datasets. Focus of this study is the assessment of different spatio-temporal wind products with a nearshore wave model. The output exhibits which wind input can pro-

vide better hindcast and forecast results for nearsbore Scotland region. For this reason the an appropriate nearshore model is selected and driven with re-analysis data, results underline expected differences in wave conditions produced from different wind products.

The choice of a nearshore numerical model, Simulating WAves Nearshore (SWAN) model, (Delft, 2014a), was based on the fact, that majority of offshore and marine energy applications is intended in depths not exceeding 150m (Waveplam, 2009; Carbon Trust and AMEC, 2012). Thus, a detailed solution of the nearshore physics is required, something that is not often met at larger oceanic models. Although approximations exist, SWAN has been validated and shown to work well for nearshore and medium scale models (shelf seas) (Akpinar and Kömürcü, 2013; Bunney, 2011; Janssen, 2008; Booij et al., 1999).

Results are useful for numerical wave modelling, by identifying the performance of different wind products and validating the data against buoy measurements. Indicating the selection of most appropriate dataset for nearshore modelling in Scotland, and expected behaviour based on wind inputs. Enhancing confidence in the data outputs, and allowing for modelled data to be considered even at location where not buoys exist.

2. Numerical Model

Knowledge in evaluation of wave resource assessments has been improving over the years, with new computational advancements and wave theory re-formulations in numerical models. From the Airy's theory of small amplitude waves in finite environments, to Miles generation of waves and Janssen's improvements on wind generated waves, the understanding of waves has improved significantly (Janssen, 2009; Holthuijsen, 2007). However, waves do not follow linear wave theory and their nature is far more complex. To overcome this, numerical models have been applied to resolve non-linearity of waves. Numerical models such as WAve Model (WAM) (WAMDI, 1988; Komen et al., 1994), and WaveWatch 3 (WW3) (Tolman and development Group, 2014) have been used for oceanic applications. For nearsore applications with shallow water SWAN and MIKE21 are often preferred (Delft, 2014a; Venugopal et al., 2010).

SWAN is a third generation model, developed by Delft University,(Delft, 2014b), as the necessity of the solving nearshore environments increased (WAMDI, 1988). Numerical wave models can be separated in stochastic

or deterministic, implicit or explicit, SWAN is a phase-averaged model that resolves the action balance equation in Cartesian or Spherical coordinates. Additionally, nearshore physics are enhanced with approaches that are often not included in larger models, due to increase of computational demands (Holthuijsen, 2007; Delft, 2014b). For simple computations Cartesian stationary computations are advised.

The action balance equation in SWAN is solved in terms of radian frequency (σ) with all shallow water physics attributed. The wave kinematic equation is given in a non-stationary (t) solution, with Spherical coordinates of latitude (λ) and longitude (φ), frequency (σ), direction (θ) and group velocities in both latitude and longitude (C_g).

$$\frac{\partial N(\sigma;\lambda;\theta;t)}{\partial t} + \frac{\partial C_{g,\lambda} N(\sigma;\lambda;\theta;t)}{\partial \lambda} + \cos\phi^{-1} \cdot \frac{\partial C_{f,\phi} N(\sigma;\lambda;\theta;t)}{\partial \phi} + \frac{\partial C_{f,\theta} N(\sigma;\lambda;\theta;t)}{\partial \theta} + \frac{\partial C_{f,\sigma} N(\sigma;\lambda;\theta;t)}{\partial \sigma} = \frac{S(\sigma;\theta;\lambda;\varphi;t)}{\sigma} \quad (1)$$

SWAN source terms allow for multiple physics to be implemented in the calculations, with detailed nearshore water components distinguishing SWAN from its oceanic counterparts. By taking into account complex terms of dissipation, bottom friction, depth breaking, triad interactions, diffraction, and diffusion the results can provide a more accurate description of the nearshore environment. Source terms Eq. 2 are: wind input (S_{in}), triads (S_{nl3}), quadruplet (S_{nl4}) interactions, whitecapping ($S_{ds,w}$), bottom friction ($S_{ds,b}$) and ($S_{ds,br}$) depth breaking. Additionally all the terms allow a wide range of computational alternatives, based on research and experiments (Delft, 2014a).

$$S_{tot} = S_{in} + S_{nl3} + S_{nl4} + S_{ds,w} + S_{ds,b} + S_{ds,br} \quad (2)$$

In our model S_{in} is based on Janssen's exponential growth theory, which has been incorporated in the $WAM4$ distribution (Janssen, 1991). Quadruplet interactions S_{nl4} are activated with a semi-explicit solution, and S_{nl3} are also activated. Both these terms are important to be considered since they represent the exchange of frequencies between waves and wind (S_{nl4}), as they propagate from deep to shallow water (S_{nl3}). Thus allowing the exchange of frequencies to be resolved and the energy re-distributed (Hasselmann et al., 1985; Holthuijsen, 2007; Van Der Westhuysen et al., 2007). Bottom friction

and depth interaction terms are also enabled their coefficients in this study are tuned based on Zijlema et al. (2012). Vegetation and mud transport were not accounted for, refraction and diffraction terms were also activated.

Furthermore, apart from different physical terms chosen, several numerical changes can be made affecting the computational processes. These were mainly focused on the calculations and iteration number. Alteration in the re-computation use of the boundary conditions were used, SWAN re-computes the incoming boundary waves, thus a criteria was set for difference between the incoming waves and re-computed ones, not to exceed 5% than the boundary inputs.

3. Model Set-up and Modelling Process

The main objective of this work is to establish the optimal selection of wind input for the region of Scotland. The assessment of wind data, is focused at the North Sea area (East of Scotland) and the Outer Hebrides (West of Scotland), see Fig. 1. The Outer Hebrides are exposed to the Atlantic and thus its boundaries are more exposed to swells and strong wind. Swells from the North Sea also occur mainly from the Northern bounday, however their intensity is relatively weaker in comparison to the North-West Atlantic swells. In order to include long distance swells into the model domain, wave boundary conditions are constructed and applied to the model.

3.1. Bathymetry and Model Domain

Bathymetric data were extracted from NOAA's database ETOPO1 (Amante and Eakins, 2014), using the 1 arc minute bathymetry is used to produce a regular mesh with spatial resolution of 0.025^o. The detailed bathymetry allows for better simulation of the neashore water physics such as dissipation and triads, although the computational demands are increased.

The bathymetry shown in Fig. 1 exhibits differences between two coastlines (East and West of Scotland). The bathymetry changes significantly for the West part, with expected conditions to be both deep and coastal water. On the other hand, the East side of the Scottish coastline has a depth profile rather constant across the East Side $\approx 50m$ for deeper locations.

3.2. Boundary Input

Two wind fields have been used for this wave modelling work. The ERA-Interim Re-Analysis wind was obtained form the European Centre for

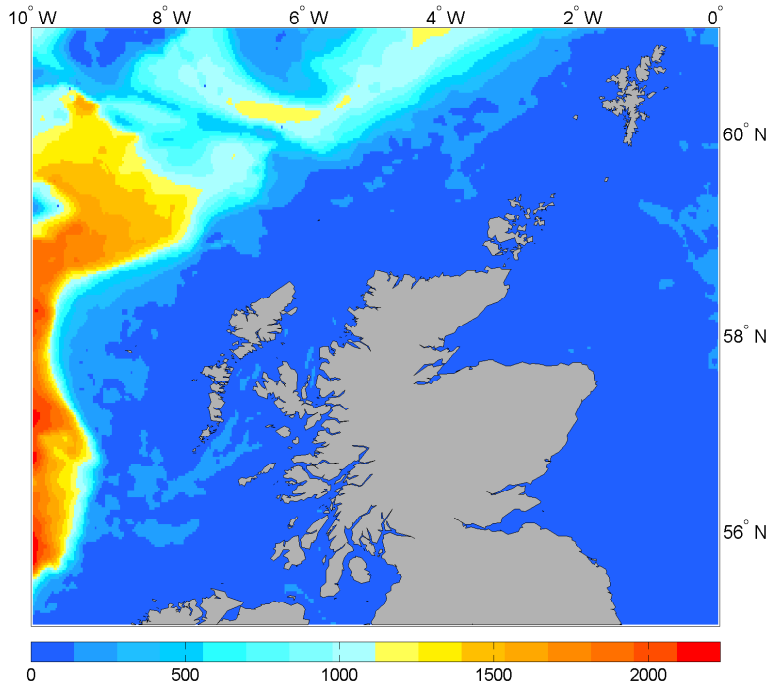

Figure 1: Mesh domain, depth is in meters(m)

Medium Weather Forecasts (ECMWF), has a spatial resolution of 0.125^o and is available for 6-hours temporal resolution (Dee et al., 2011). The second wind product is the Climate Forecast System Reanalysis denoted henceforth as $CFSR$, provided by the National Centre for Environmental Prediction (NCEP) (Saha et al., 2010). It offers 1-hour time-steps, with a spatial resolution 0.3^o. For both products parameters extracted are wind speeds zonal (U_{10}) and meridional (V_{10}), corresponding to 10m height above mean sea level. Which were formatted to a suitable input format to be assimilated in SWAN, based on the corresponding spatial resolution.

Data included at CFSR dataset are products from several re-analysis tests at NCEP, with period of availability from 1979-2010, for those characteristics. Experimental comparisons have shown that the latest products have increase their accuracy , in comparison with previous releases (Stopa et al., 2013).

The European Centre for Medium-Range Forecasts (ECMWF), offers wind data with various spatial resolution spanning from 0.125^o up to 3°. Some issues have been identified in regards to ECMWF underestimation of U_{10}, but constant upgrades are performed with the latest at the end of June

2013. This alleviated older problems by previous re-analysis, especially after 2010 new models were used to improve the fields for 2010-2011. The temporal resolution available are 6-hr (public domain) 3-hr and 1-hr (under permission) (Richardson et al., 2013).

SWAN requires initial spectral quantities to be assigned and after assessment of previous hindcasts in the area, (Lavidas et al., 2014) screening of the areas frequency bins and directions were given. Minimum frequency was set to 0.04 Hz and maximum at 1 Hz with 24 frequency bins, and 24 directional bins used. In addition to wind input, wave boundary conditions were also extracted from the ECMWF spectral database, and files where created for the boundary conditions in SWAN, with Significant wave height (H_s) in meters, Peak period (T_p) in seconds, Peak Direction (P_kDir) in degrees, and Directional Spreading (D_{spr}) in degrees recorded at 6-hourly intervals. The above boundary information obtained from ECMWF were isolated at specified point locations. In order to correctly apply them on the model boundaries, the boundary lines were divided into several small sections of 1° and then the corresponding wave input data were applied as boundaries.

3.3. Model Implementation

SWAN relays on solving Eq. 1 for all the components of the Eq. 2, in regards with the boundary and wind input. The area covered is one quadrant per time, for the computational step given, see Fig. 2, thus time resolution will not only play a role in the step chosen but also in the accurate calculation of the wave parameters and not increasing the computational requirements.

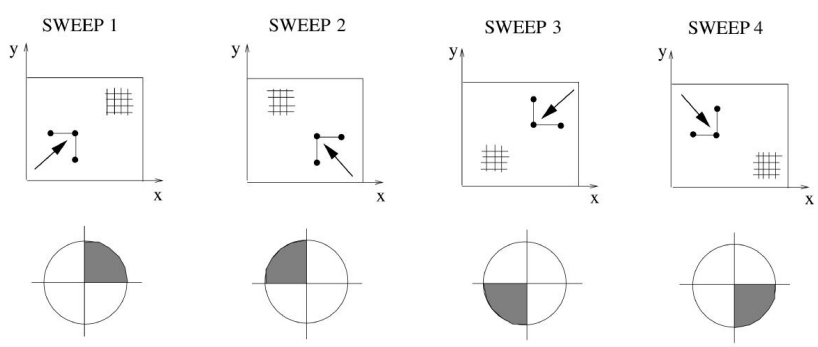

Figure 2: Iterative solution procedure for the wave energy by SWAN (Delft, 2014a)

This means that after each propagation at a geographic grid point, SWAN updates wave and spectral components and "inserts" them into the next iteration, alongside with the wind information of that cell. The upwind component is responsible for determination on the spectral balance equation and propagated energy. Thus, resolution of wind fields is of major concern that affects not only the generation trend but also magnitude, propagation velocities, and spectral shape.

Both wind products considered for this work run in the same SWAN code, with selected physics custom for the area and activated as referred in Section 2. Attention has been given in incorporating all the physical elements that affect wave resource, whilst minimizing the irregular behaviour by alternating and changing key terms such as the re-computation of the boundary points and physical interactions (Zijlema et al., 2012; Rogers et al., 2002; Dietrich et al., 2012).

4. Calibration and Validation of the Models

An initial small period was initially used to calibrate the model (Lavidas et al., 2014). The results showed promise and established confidence that the model can be extended for an annual run with the expectation of good correlated results. Indicatively, correlation coefficients for two buoys located in the West Scottish coastlines, were 0.98 and 0.97 for H_s. Similar behaviour was presented for the peak period with coefficients from $0.92 - 0.94$. Biases in the calibration process remained low for all quantities, see Figs. 3-4.

It has been recorded in several cases, the coastal H_s being rather small, by having multiple benchmarks one can assess the performance of the model. In Ris et al. (1999) the example of combining variable indexes was used, it was stated that even if the rms is low a SI parameter may be extremely high, something that will decrease the reliability of the model by missing peaks or troughs. In Eqs 3-8 all statistical indices used for the comparison of modelled results with buoy data are presented.

$$bias = \sum_{i=1}^{N} \frac{1}{N}(X_i - Y_i) \tag{3}$$

$$rms = \sqrt{\frac{1}{N}\sum_{i=1}^{N}(X_i - Y_i)^2} \tag{4}$$

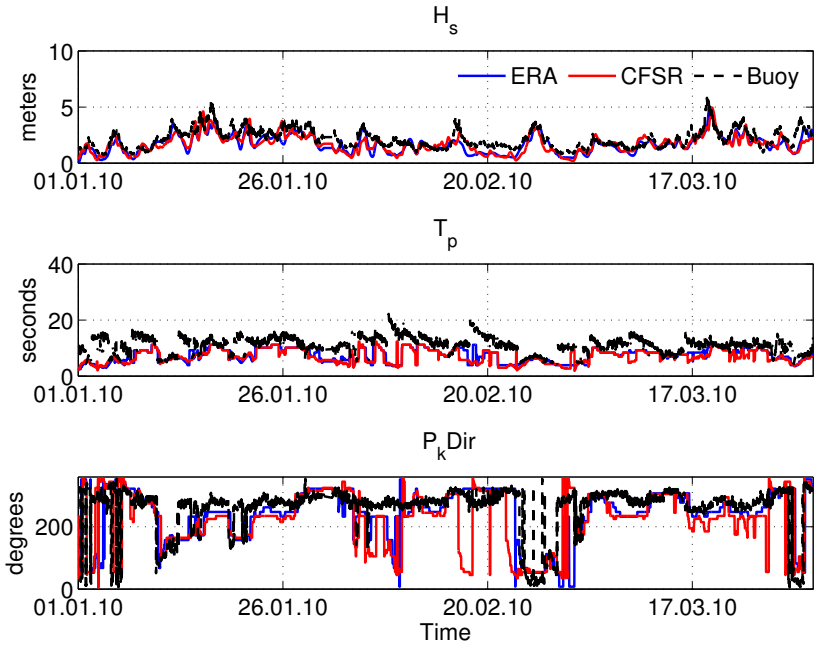

Figure 3: Calibration of Blackstone buoy

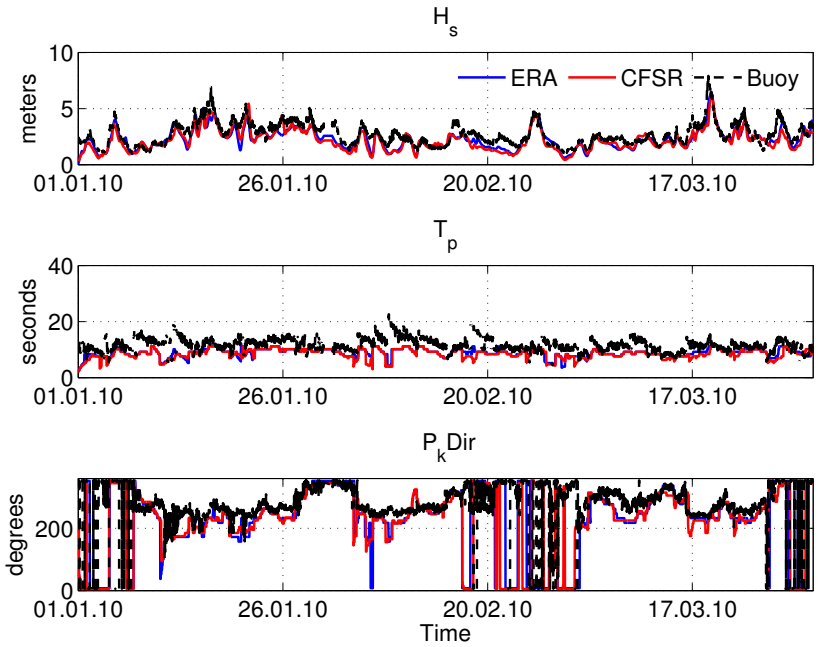

Figure 4: Calibration of West Hebrides buoy

$$R = \frac{\sum_{i=1}^{N}((X_i - \overline{X_i})(Y_i - \overline{Y_i}))}{\sqrt{((\sum_{i=1}^{N}((X_i - \overline{X_i})^2)((\sum_{i=1}^{N}((Y_i - \overline{Y_i})^2)}} \tag{5}$$

$$SI = \frac{rms}{\frac{1}{N}\sum_{i=1}^{N} Y_i} \tag{6}$$

$$MPI = |1 - \frac{rms}{rms_{change}}| \tag{7}$$

$$rms_{change} = \sqrt{\frac{Y_i^2}{N}} \tag{8}$$

where X_i is the simulated wave parameter, Y_i the buoy wave quantity, N measurements. The rms_{change} is similar to the use of rms but the data we take into consideration are only the observed. The use of several quantitative indices will allow better classification, for example in some cases we may obtain a good bias, small SI and a moderate MPI. Thus, by incorporating more methods available, a correlation of the simulated and observed values can be established (Ris et al., 1999; Komen et al., 1994). For these hindcasts the H_s, T_p and T_z are compared with all the values.

A quantitative approach is used to determine accuracy between the different results and the buoy, allowing us to expand and investigate the wind product effects. Quantitative metrics for comparing model results will be the bias parameter, the root mean error (rms), correlation coefficient (R), Scatter Index (SI) and model performance (MPI) indexes, as well as the distributions obtained. The rms value is normalized with the observed and simulated results over the duration of the data available, this will ensure a proper comparison of SWAN simulations either they are performed in small coastal areas, or bigger domains.

5. Results

The year of the hindcast is 2010, where buoys have available comparison data. Buoy measurements are used to assess the quality of hindcasts. Since CFSR and ECMWF have different temporal and spatial resolution it is important to quantify the differences between their modelled results and assess

their accuracy. Numerical physical terms are set the same for both runs minimizing potential non-similarities in final results. Assessment is carried with the comparison of wave data to recorded wave conditions at specified locations (CEFAS, 2014), compared annually and seasonally divided with hindcast duration of 1-year in both cases.

The area under investigation is given in Fig. 1, four buoys under investigation are located at the West and East side of Scotland, results are given in terms of West and East side of Scotland, with four buoys in total two at each side. Buoys are located at West Hebrides, Blackstone, Firth of Forth and Moray Firth (CEFAS, 2014). Buoys were operated for 2010 recording wave parameters and spectral data for 30 minutes intervals.

In Table 1 presents mean values for buoys and hindcast results, it has to be noted that buoy recordings have missing data for some time intervals. For this reason a post processing was applied to consider only recorded data measurements for comparison. Annual results present similar trends as in Stopa and Cheung (2014), whose work included a significantly larger dataset and focused in the North American region. Their results also suggest that CFSR wind have overestimations and higher scatter in contrast to ECMWF. From our sub-sequent analysis similar trends are identified, though some areas perform better pending on dataset.

From Figures 5-8 corresponding hindcast intervals are presented, it is noticeable that in all cases generation trend shows good agreement. CFSR dataset shows larger "peaks" than the corresponding buoy time-series. Table 1 shows the biases between hindcasts and wave parameters. CFSR have consistently model higher H_{sig}, and lower periods (T_p, T_z). Resulting in general over-estimation performance for H_{sig} and underestimations for periods.

Table 1: Annual Indexes for the wind datasets

	West Hebrides						Blackstone					
	H_s in m		T_p in sec		T_z in sec		H_s in m		T_p in sec		T_z in sec	
	ECMWF	**CFSR**	**ECMWF**	**CFSR**	**ECMWF**	**CFSR**	**ECMWF**	**CFSR**	**ECMWF**	**CFSR**	**ECMWF**	**CFSR**
Average Buoy	2.25	2.25	9.90	9.90	6.23	6.23	2.02	2.02	9.72	9.72	5.96	5.96
Average SWAN	1.93	1.99	10.15	9.93	6.02	5.81	1.93	2.16	9.55	8.99	5.95	5.61
	Firth of Forth						Moray Firth					
	H_s in m		T_p in sec		T_z in sec		H_s in m		T_p in sec		T_z in sec	
Average Buoy	1.14	1.14	7.03	7.03	4.53	4.53	1.12	1.12	7.14	7.14	4.37	4.37
Average SWAN	0.97	1.47	8.08	7.02	5.20	4.6	0.90	1.11	8.08	7.23	4.65	4.40

To further assess performance annual measurements are separated in seasons and compared with buoys. This allows examination and corresponding effects winds have on seasonal hindcast. From January 1st until April 1st is denoted as Season 1, April 1st to July 1st as Season 2, July 1st to October 1st

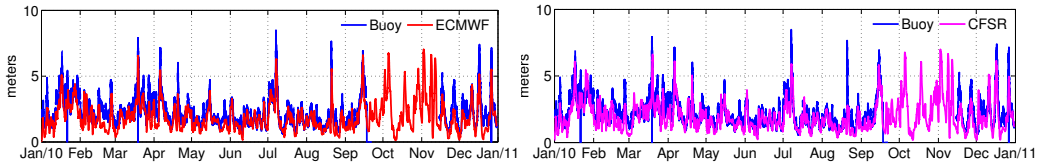

Figure 5: Annual H_s timeseries at West Hebrides buoy with both wind products

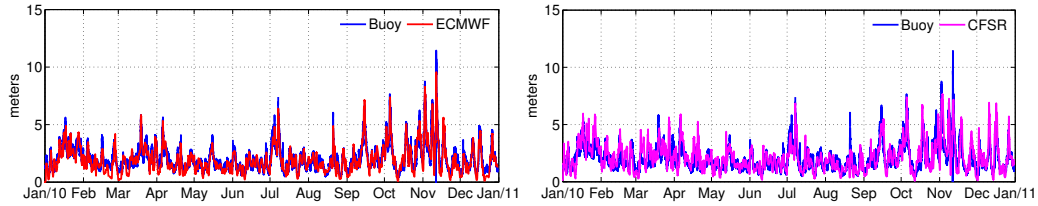

Figure 6: Annual H_s timeseries at BlackStone buoy with both wind products

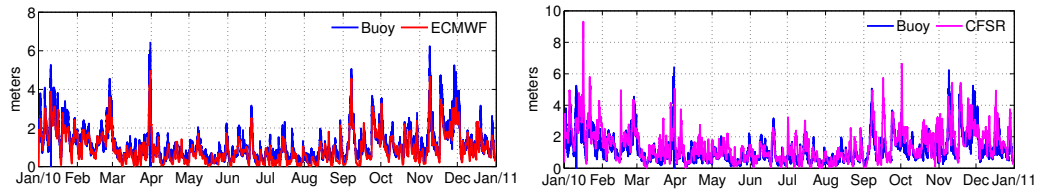

Figure 7: Annual H_s timeseries at Firth of Forth buoy with both wind products

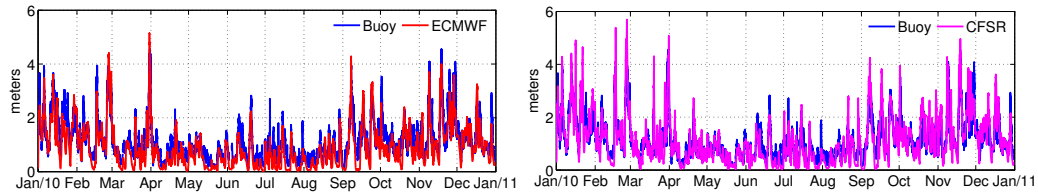

Figure 8: Annual H_s timeseries at Moray Firth buoy with both wind products

as Season 3 and by October 1st until December 31st as Season 4. Following the evaluation and a further understanding of the affected physical terms is presented. Tables 3-5, performance indices for the model results and buoy, based on the different datasets. Although the dissemination of the results are given for every buoy based on the characteristics that affect the performance of the model.

In Figs. 9-10, the levels of incoming swells are shown. In both cases

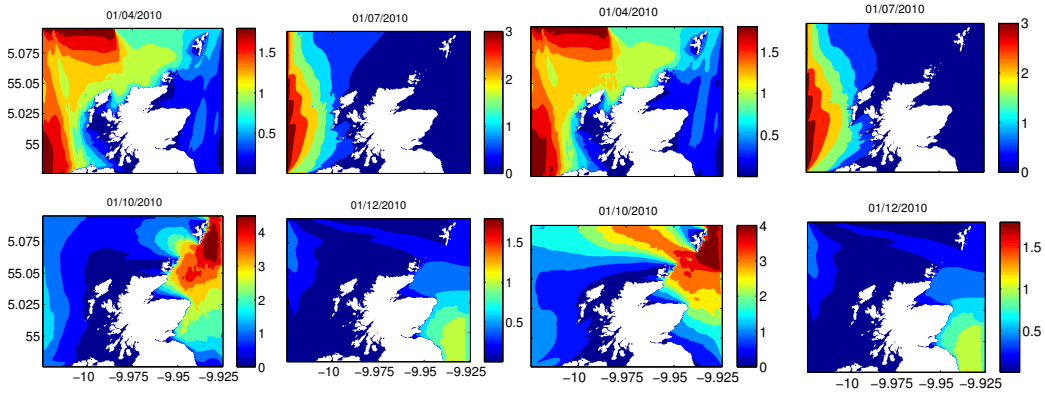

Figure 9: H_{swell} (m) for $CFSR$ dataset

Figure 10: H_{swell} (m) for $ECMWF$ dataset

trends and fields have similar tracks, however magnitude for swell quantities is slightly different. CFSR data tend to have similar magnitudes in their H_{swell} components, however high swell areas covered are extended for CFSR winds. Exposed boundaries of the location shown in Figs. 9-10, illustrate the effect of wave boundary originating from the Atlantic, a highly volatile environment that is inhabited by both wind seas and distant generated swells. These incoming components affect the final wave energy resource of the area, and their propagation is affected by the wind input.

First buoy analysed is the Blackstone buoy, located at the West Side of the Scottish coastline near the Isle of Islay at 97 meters depth and operational from March 2009 until present (CEFAS, 2014). In Table 2, Fig. 6 and Figs. 11-12, the results for wave parameters used to characterise the performance are presented. The buoy is located at intermediate to shallow waters, meaning that triad non-linear interactions play a significant role in the alteration of the wave field, the physics for which have been activated accordingly. The correlation coefficient R and MPI are high for both models, the temporal improvement shows no alteration on the numerical solver of SWAN. In fact the ECMWF dataset produces a slightly higher performance for the quantities.

Seasons 1 and 4 (autumn and winter) have the highest average range of H_s. Wind input by ECMWF presents underestimations for all seasons, however biases are fairly small, with Season 3 hindcasting almost no bias. The situation is different for CFSR hindcast. The increased temporal resolution of the dataset led to higher peaks and overestimations (seasonal), as it can

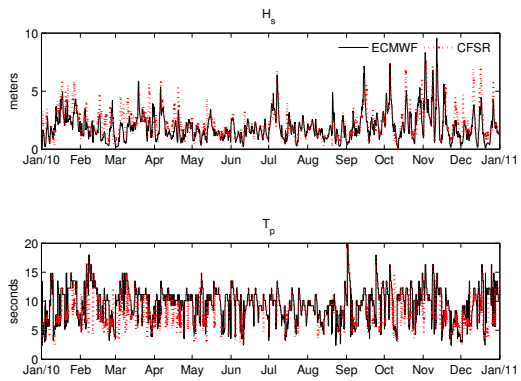

Figure 11: H_s and T_p at Blackstone

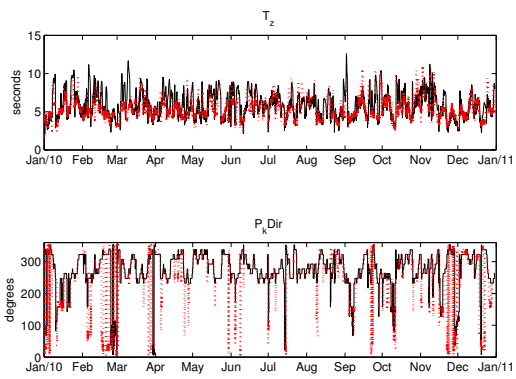

Figure 12: T_z and P_kDir Blackstone

be seen by the rms and a higher Scatter Index (SI). This may be expected when the wave resource is at its peak, during winter months, although the driving wind shows the same results for the "less" energetic summer seasons.

Periods T_z and T_p exhibit similar high correlation coefficients, with both models slightly underestimating the periods for winter and autumn (Season 3). In contrast to CFSR behaviour, ECMWF driven waves are overestimating the spring and summer months (Season 3). No significant differences exist and overall performance can be classified as high. In general CFSR data attain higher peaks leading to overestimations, while ECMWF driven data present lower differences and significantly lower SI.

Table 2: Blackstone Seasons Indexes

	Blackstone											
	Season 1						Season 2					
	H_s		T_p		T_z		H_s		T_p		T_z	
	ECMWF	**CFSR**	**ECMWF**	**CFSR**	**ECMWF**	**CFSR**	**ECMWF**	**CFSR**	**ECMWF**	**CFSR**	**ECMWF**	**CFSR**
Correlation	0.96	0.93	0.93	0.96	0.97	0.96	0.96	0.93	0.95	0.94	0.97	0.96
Average Buoy	2.15	2.15	10.47	10.47	6.24	6.24	1.64	1.64	9.71	9.71	5.94	5.94
Average SWAN	1.97	2.39	9.94	8.87	6.10	5.40	1.56	1.81	9.58	9.16	6.08	5.68
Bias	-0.18	0.24	-0.53	-1.6	-0.13	-0.83	-0.08	0.17	-0.13	-0.54	0.14	-0.26
rms	0.51	0.92	3.54	4.25	1.34	1.45	0.35	0.62	2.45	2.8	1.04	1.28
SI	0.24	0.42	0.33	0.40	0.21	0.23	0.21	0.38	0.25	0.28	0.17	0.21
MPI	0.96	0.96	0.84	0.84	0.90	0.90	0.97	0.97	0.85	0.85	0.91	0.91
	Season 3						Season 4					
	H_s		T_p		T_z		H_s		T_p		T_z	
	ECMWF	**CFSR**	**ECMWF**	**CFSR**	**ECMWF**	**CFSR**	**ECMWF**	**CFSR**	**ECMWF**	**CFSR**	**ECMWF**	**CFSR**
Correlation	0.96	0.93	0.95	0.94	0.96	0.95	0.96	0.93	0.92	0.91	0.96	0.95
Average Buoy	1.90	1.90	8.90	8.90	5.59	5.59	2.39	2.39	9.78	9.78	6.07	6.07
Average SWAN	1.90	1.85	8.92	8.86	5.77	5.76	2.30	2.59	9.75	9.06	5.84	5.59
Bias	0.00	-0.05	0.02	-0.04	0.18	0.17	-0.09	0.20	-0.03	-0.72	-0.23	-0.48
rms	0.38	0.66	2.28	2.49	1.16	1.31	0.53	0.94	3.54	3.75	1.28	1.48
SI	0.19	0.34	0.25	0.28	0.20	0.23	0.22	0.39	0.36	0.38	0.21	0.24
MPI	0.97	0.97	0.86	0.86	0.91	0.91	0.96	0.96	0.85	0.85	0.91	0.91

The Hebrides buoy is also located alongside the West Scottish coastline,

specifically the South part of the Island of Lewis, at 100 meters depth and operational since 2009 (CEFAS, 2014). Both the West Hebrides and Blackstone are located at the Atlantic side of Scotland, which involves higher values of incoming waves and significant amounts of swells. The high wind resource of the area constantly affects directionality of waves, local winds provide an additional source of "young" seas generation, which are be combined with incoming swells.

As seen in Table 3 highest average values of H_s are recorded for winter months. Correlation coefficient is good for both wind driven models. However, increased temporal resolution offers smaller biases for CFSR data with similar SI and rms errors, see Fig. 5 and Figs. 13-14.

Table 3: West Hebrides Seasons Indexes

-	West Hebrides											
	Season 1						**Season 2**					
	H_s		T_p		T_z		H_s		T_p		T_z	
	ECMWF	**CFSR**	**ECMWF**	**CFSR**	**ECMWF**	**CFSR**	**ECMWF**	**CFSR**	**ECMWF**	**CFSR**	**ECMWF**	**CFSR**
Correlation	0.95	0.95	0.94	0.93	0.96	0.96	0.95	0.95	0.96	0.95	0.96	0.96
Average Buoy	2.69	2.69	10.89	10.89	6.83	6.83	1.98	1.98	9.89	9.89	6.21	6.21
Average SWAN	2.04	2.20	10.72	10.54	6.23	5.71	1.63	1.73	10.06	9.71	6.14	5.93
Bias	-0.65	-0.49	-0.17	-0.35	0.60	-1.12	-0.35	-0.25	0.17	-0.18	-0.07	-0.28
rms	0.88	0.86	3.58	3.71	1.55	1.83	0.54	0.54	2.05	2.35	1.01	1.25
SI	0.32	0.32	0.32	0.34	0.22	0.26	0.27	0.27	0.20	0.23	0.16	0.20
MPI	0.95	0.95	0.83	0.83	0.89	0.89	0.97	0.97	0.85	0.85	0.90	0.90
	Season 3						**Season 4**					
	H_s		T_p		T_z		H_s		T_p		T_z	
	ECMWF	**CFSR**	**ECMWF**	**CFSR**	**ECMWF**	**CFSR**	**ECMWF**	**CFSR**	**ECMWF**	**CFSR**	**ECMWF**	**CFSR**
Correlation	0.96	0.96	0.96	0.96	0.91	0.91	0.96	0.95	0.95	0.94	0.96	0.95
Average Buoy	1.99	1.99	8.59	8.59	5.53	5.53	2.38	2.38	10.30	10.30	6.34	6.34
Average SWAN	1.71	1.69	9.19	8.21	5.72	5.78	2.23	2.30	10.62	10.27	5.98	5.83
Bias	-0.28	-0.30	-0.27	0.38	0.59	0.25	-0.15	-0.08	0.32	-0.03	-0.36	-0.51
rms	0.59	0.79	0.71	5.21	2.96	1.84	0.61	0.61	2.44	2.6	1.12	1.25
SI	0.30	0.42	0.35	0.31	0.34	0.33	0.25	0.25	0.23	0.25	0.17	0.19
MPI	0.96	0.96	0.86	0.84	0.86	0.91	0.96	0.95	0.84	0.84	0.90	0.90

Period performance, as seen in Table 3 has more diverse alterations. Correlation for both models is high, Season 2-3 exhibit similar results with closely followed biases and rms. ECMWF has slightly better values this can be attributed to the higher spatial resolution. For winter months Season 1 and 4 have different results. for Season 1 both models underestimate the T_p, while CFSR also underestimate and has higher rms for all parameters. Similar performance is exhibited for T_z with CFSR driven waves presenting a constant underestimation.

The Moray Firth buoy is located at North-East of Scotland, at 54 meters depth and has been active since 2008. The area is exposed to swells originating from the North side, while the East and West boundaries are large land masses. Subsequently, swell components are not as strong as the previous areas.

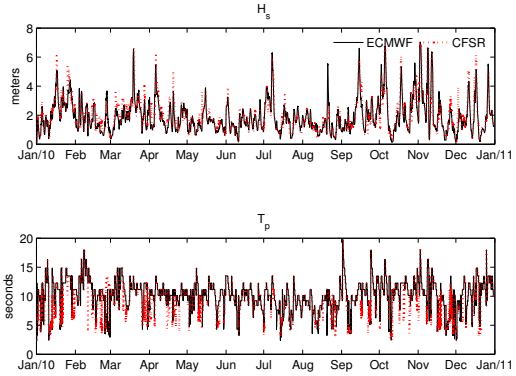

Figure 13: H_s and T_p at West Hebrides

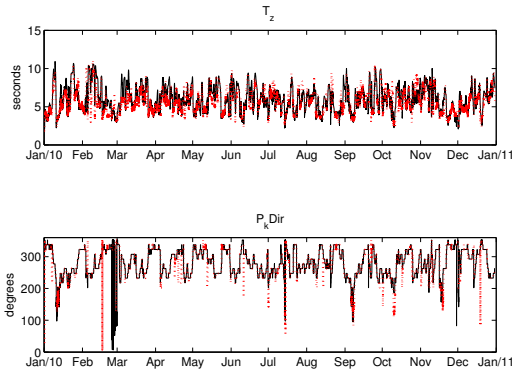

Figure 14: T_z and $P_k Dir$ at West Hebrides

Table 4: Moray Firth Seasons Indexes

	Moray Firth											
	Season 1						**Season 1**					
	H_s		T_p		T_z		H_s		T_p		T_z	
	ECMWF	**CFSR**	**ECMWF**	**CFSR**	**ECMWF**	**CFSR**	**ECMWF**	**CFSR**	**ECMWF**	**CFSR**	**ECMWF**	**CFSR**
Correlation	0.94	0.94	0.90	0.90	0.95	0.94	0.90	0.93	0.85	0.85	0.93	0.94
Average Buoy	1.47	1.47	7.96	7.96	4.89	4.89	0.72	0.72	6.58	6.58	3.96	3.96
Average SWAN	1.25	1.53	8.41	7.49	5.08	4.73	0.52	0.62	8.36	7.11	4.54	4.14
Bias	-0.22	0.04	0.44	-0.47	0.19	-0.16	-0.20	-0.10	1.78	0.53	0.58	0.18
rms	0.49	0.54	3.52	3.45	1.42	1.42	0.32	0.28	3.99	3.58	1.50	1.30
SI	0.33	0.36	0.44	0.43	0.29	0.29	0.44	0.38	0.60	0.54	0.37	0.33
MPI	0.97	0.97	0.87	0.87	0.92	0.92	0.98	0.98	0.90	0.90	0.94	0.94
	Season 3						**Season 4**					
	H_s		T_p		T_z		H_s		T_p		T_z	
	ECMWF	**CFSR**	**ECMWF**	**CFSR**	**ECMWF**	**CFSR**	**ECMWF**	**CFSR**	**ECMWF**	**CFSR**	**ECMWF**	**CFSR**
Correlation	0.91	0.92	0.86	0.85	0.94	0.94	0.93	0.94	0.89	0.89	0.95	0.95
Average Buoy	0.91	0.91	6.14	6.14	3.99	3.99	1.37	1.37	7.86	7.86	4.63	4.63
Average SWAN	0.67	0.84	7.42	6.71	4.29	4.20	1.17	1.46	8.11	7.59	4.69	4.54
Bias	-0.25	-0.07	1.28	0.56	0.30	0.20	-0.20	0.09	0.25	-0.27	0.06	-0.09
rms	0.42	0.40	3.84	3.64	1.27	1.29	0.44	0.46	3.45	3.59	1.14	1.04
SI	0.45	0.44	0.62	0.59	0.31	0.32	0.31	0.33	0.43	0.45	0.24	0.22
MPI	0.98	0.98	0.90	0.90	0.94	0.94	0.97	0.97	0.88	0.88	0.93	0.93

In this partially "enclosed" environment generation of waves by the wind, is satisfactory with correlation indexes over 0.9, while the model performance MPI presents a very good model hindcast. Improved temporal resolution of CFSR shows better performances. Specifically for H_s, all seasonal rms errors have very close agreement, with ECMWF data presenting larger underestimation when compared with CSFR biases, see Fig. 8 and Figs 15-16.

In all cases differences are in favour of CFSR wave data with reduced average biases, see Table 4. period T_z has similar results with good correlation factors and high MPI. On the other hand, the correlation of the T_p is above 0.85 for both fields, though it shows that CFSR consistently perform better than the ECMWF with both models usually overestimating, see Table 4.

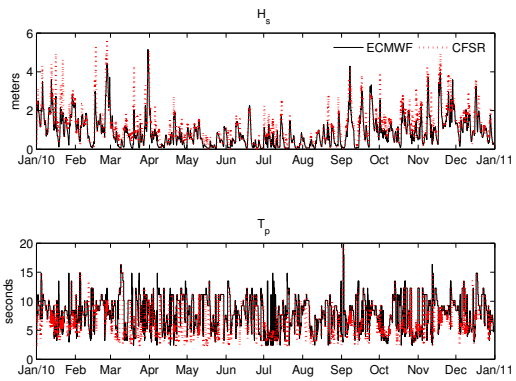

Figure 15: H_s and T_p Moray Firth

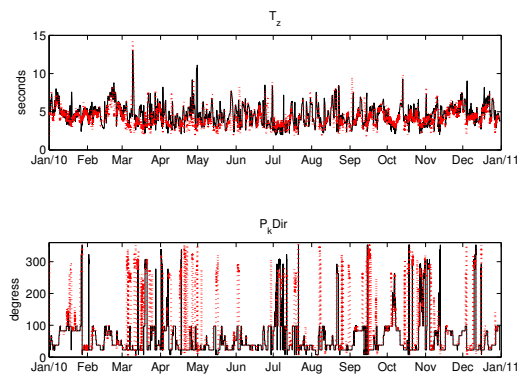

Figure 16: T_z and P_kDir at Moray Firth

Due to the enhanced temporal resolution, the bias presents almost 50% less than ECMWF, while the overall rms and SI indices are in favour of the CFSR.

Final location under consideration, Firth of Forth, the buoy is at 65 meters depth and the site is located at the middle portion of Scotland, just outside of Edinburgh. The location has similar characteristics as the Moray Firth, with swell originating from the North boundary. The detailed indexes are given in Table 5.

Table 5: Firth of Forth Seasons Indexes

	Firth of Forth											
	Season 1						**Season 2**					
	H_s		T_p		T_z		H_s		T_p		T_z	
	ECMWF	**CFSR**	**ECMWF**	**CFSR**	**ECMWF**	**CFSR**	**ECMWF**	**CFSR**	**ECMWF**	**CFSR**	**ECMWF**	**CFSR**
Correlation	0.97	0.89	0.94	0.93	0.96	0.95	0.94	0.87	0.89	0.88	0.93	0.94
Average Buoy	1.50	1.50	8.08	8.08	5.16	5.16	0.71	0.91	6.47	6.47	4.05	4.05
Average SWAN	1.32	1.91	8.87	7.78	5.81	5.14	0.60	0.93	7.82	6.51	5.01	4.29
Bias	-0.18	0.41	0.78	-0.30	0.65	0.02	-0.11	0.22	1.35	0.04	0.96	0.24
rms	0.39	1.02	2.88	2.71	1.46	1.38	0.25	0.50	3.47	3.18	1.80	1.28
SI	0.26	0.67	0.35	0.33	0.28	0.26	0.35	0.70	0.53	0.49	0.44	0.31
MPI	0.97	0.97	0.87	0.87	0.92	0.92	0.98	0.98	0.90	0.90	0.93	0.93
	Season 3						**Season 4**					
	H_s		T_p		T_z		H_s		T_p		T_z	
	ECMWF	**CFSR**	**ECMWF**	**CFSR**	**ECMWF**	**CFSR**	**ECMWF**	**CFSR**	**ECMWF**	**CFSR**	**ECMWF**	**CFSR**
Correlation	0.94	0.86	0.90	0.91	0.95	0.95	0.97	0.89	0.91	0.92	0.96	0.96
Average Buoy	0.88	0.88	6.24	6.24	4.11	4.11	1.46	1.46	7.55	7.55	4.79	4.79
Average SWAN	0.71	1.10	6.95	6.11	4.55	4.21	1.24	1.95	8.69	7.67	5.44	4.95
Bias	-0.17	0.22	0.71	-0.13	0.44	0.11	-0.22	0.49	1.14	0.12	0.64	0.16
rms	0.32	0.69	2.99	2.50	1.29	1.14	0.38	0.95	3.34	2.80	1.40	1.01
SI	0.37	0.78	0.47	0.40	0.31	0.27	0.26	0.65	0.44	0.37	0.29	0.21
MPI	0.98	0.98	0.90	0.90	0.93	0.93	0.97	0.97	0.88	0.88	0.92	0.92

This location has smallest wave recordings, due to its location most waves are dissipated and swells are not as strong as in the West part. However, the winter-autumn season still present the highest recorded resource. In contrast

to Moray Firth, performance of CFSR is lower than ECMWF, MPI is similar for both models but ECMWF presents less errors and has smaller biases. H_s is overestimated for all seasons with CFSR, ECMWF underestimates H_s value very close to buoy mean. For all seasons SI of CFSR is underperforming significantly, see Fig. 7 and Figs. 17-18.

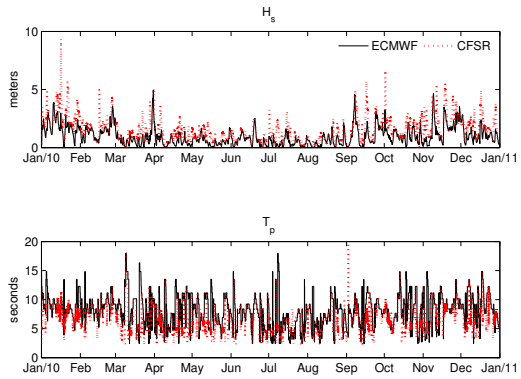

Figure 17: H_s and T_p at Firth of Forth

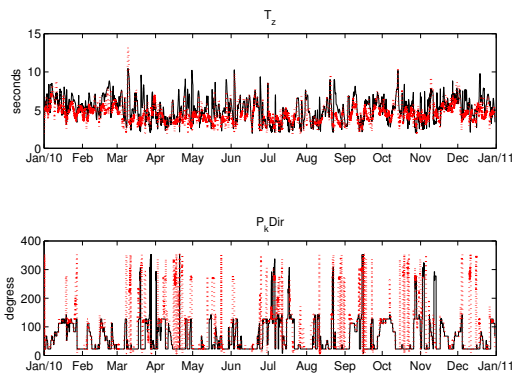

Figure 18: T_z and P_kDir at Firth of Forth

The periods T_p and T_z have better performance with the CFSR field. The higher temporal resolution allows for quicker directional information and at such coastal waters, temporal effects improve the periods measured. The rms period errors are substantially lower with the CFSR while the SI are reduced.

The underestimations and overestimations that occur with the use of different wind datasets affect not only the hindcast but the distributions of the modelled data. As showed earlier in this section, the performance of the model depends not only on the winds but the location characteristics as well. The combination of shallow water physical aspects and the wind set selection will ultimately reduce or increase the accuracy of the probability distribution for the measured quantities. In Fig. 19 the ECMWF wave driven model results exhibit better performance, with scatter diagram values having a closer correlation to measured data. The overall behaviour of ECMWF wind product, although it offers persistence in underestimations, shows that the quality of their errors is reduced leading to less discrepancies.

In Fig. 20, similar behaviour is expressed. The nearshore water physical activities in the region increase the scattering possibility throughout the year as more non-linear terms such as diffusion and refraction affect the waves.

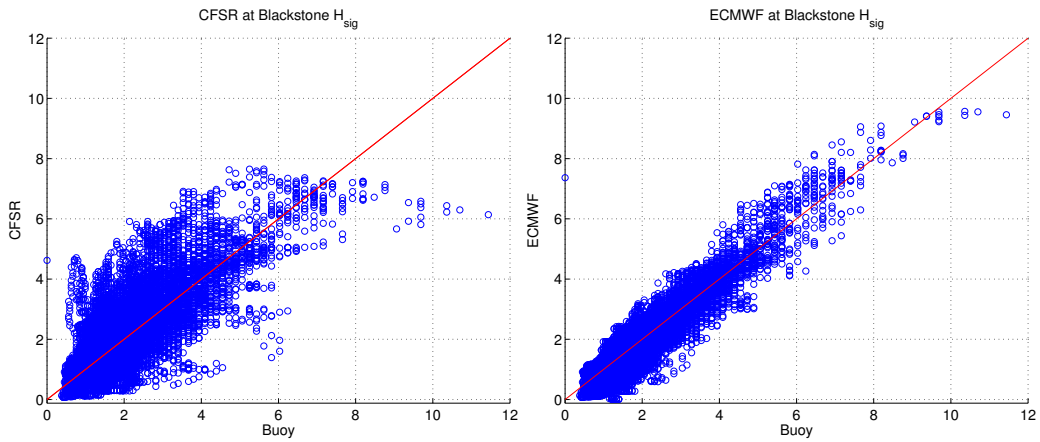

Figure 19: Scatter diagrams for Blackstone $CFSR$ (left panel), and $ECMWF$ (right panel)

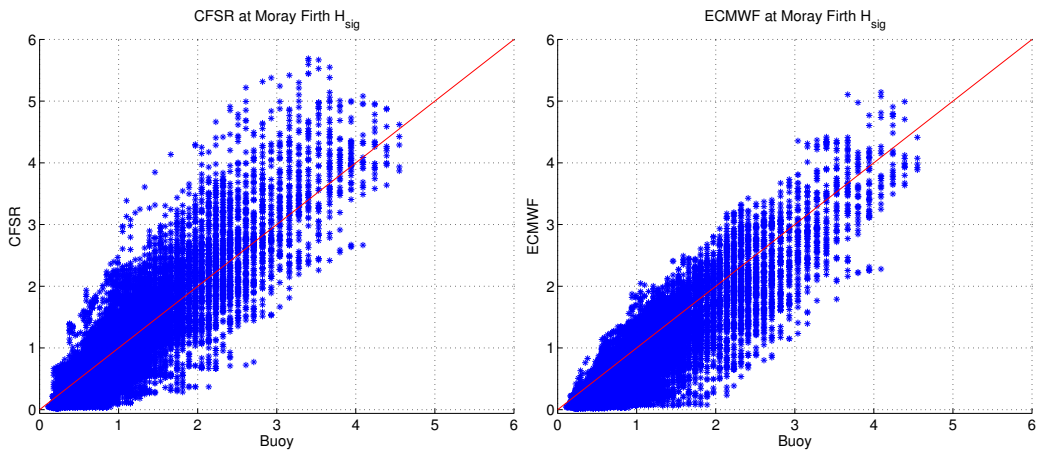

Figure 20: Scatter diagrams for Moray Firth $CFSR$ (left panel), and $ECMWF$ (right panel)

Even at nearshore environments the SWAN H_s given by the driven ECMWF winds, presents smaller annual bias although their maxima values are smaller. CFSR due to their temporal resolution generate a "peakier" environment with more changes in the maximum and minimum parameters.

6. Discussion

In the work Sterl et al. (1998), ECMWF sets were validated against recorded wind and through the use of WAM oceanic numerical model, in

order to assess wind quality. The application of WAM revealed underestimations but not in a consistent way. The overall performance of the set showed improved wind fields, though it was evident that not every area was behaving in an expected manner. Suggestions were made, in reference, to usage and increase of temporal resolution, and would perhaps lead to the increase of the accuracy and reduce biases. Caires et al. (2004) investigated differences of wind products and numerical wave models at a global scale. Same locations showed different biases and scatter indices, Several over and underestimation were present for same locations, depending on the wind dataset used. The authors concluded, that the wind datasets affect significantly the potential wave performance, and the selection of the appropriate of a dataset is not a trivial process. Different oceanic locations and global positions, may require tailored approaches.

It has been proposed that the use of a higher temporal wind input scheme improves the actual forecasts (Cavaleri, 2009) although optimizing only based on temporal inputs is not sufficient. In this study we considered to different re-analysis spatio-temporal wind dataset, coupled with the SWAN model. The hindcact quantities were shown to be highly dependent on the wind input characteristics. In our study both hindcast datasets, showed a good generation and correlation of quantities. However, as Cavaleri and Bertotti (2006); Cavaleri (2009) discussed that also spatial resolution of the input wind data alters hindcast results. This meant that pending on our location West or East of Scotland, performance varied. CFSR showed a tendency to over-estimate H_s but had lower performance in rms and larger SI. On the other hand the ECMWF wind driven dataset showed higher under-estimation of H_s, but improved SI and periods performance.

7. Conclusions

This study was focused on the assessment of different wind datasets for use in numerical wave modelling that strongly depend wind attributed. The use of SWAN custom for coastal areas allows to display the effects of wind in nearshore applications. SWAN proves to be a reliable source for reproducing complex seas, discrepancies are mainly dependent on the quality and behaviour of the wind used.

Different spatio-temporal wind dataset are used. The interaction of winds and the generated waves reveals differences in hindcast for each of the datasets. Influence of temporal and spatial resolution is very important for wave re-

source assessment, thus the selection of a proper wind field would optimise and increase the confidence in the hindcast or future forecasted waves. CFSR data have a high temporal resolution (1-hr) in contrast with the ECMWF (6-hr). Results revealed that for the West coastline area of Scotland, the ECMWF outperform its counterpart hindcasting the wave resource, with smaller biases, low rms errors and less scattering. The 6-hourly ECMWF wind inputs data show an trend in underestimating the wave resource (H_s) presenting lower peaks.

East side of Scotland although exposed to high wind resource, has "enclosed" coastline characteristics. For Moray Firth seasonal hindcast favours CFSR that outperformed the ECMWF model. Indices showed that ECMWF consistently underestimates H_s with peak T_p slightly overestimated.

Numerical wave modelling is dependent on the quality of wind data, results revealed a trend that seems to appear in both datasets. Overall for the region of Scotland and North Sea, ECMWF data present better hindcast results for the region. ECMWF driven numerical wave model exhibits lower differences with recorded wave, and although H_s are underestimated SI and biases are smaller and closer to buoy measurements.

This does not reduce the performance of CFSR data, their higher temporal resolution allowed better simulation of peaks which may be advantageous for studies concerning extreme value analysis, for engineering applications.

8. Acknowledgments

The first author would like to thank the Engineering and Physical Sciences Research Council (EPSRC) for Ph.D. funding. The authors would like to acknowledge ECMWF and NCEP for their work in the Re-analysis data provided, the development team of SWAN at TU Delft University Hydraulics Department, and thank the reviewers comments for improving the manuscript.

9. References

Akpinar, A., Kömürcü, M. ., jan 2013. Assessment of wave energy resource of the Black Sea based on 15-year numerical hindcast data. Appl. Energy 101, 502–512.

Amante, C., Eakins, B., 2014. ETOPO1 1 Arc-Minute Global Relief Model: Procedures, Data Sources and Analysis. NOAA Technical Memorandum NESDIS NGDC-24.

Bidlot, J.-R., Janssen, P., Abdalla, S., 2006. Extreme waves in the ECMWF operational wave forecasting system. In: 9th Int. Work. wave hindcasting Forecast.

Bidlot, J.-R., Janssen, P., S., A., 2005. On The Importance Of Spectral Wave Observations In The Continued Development Of Global Wave Models. In: Proc. 5th Int. Symp. Ocean Wave Meas. Anal. Madrid, june 2005. pp. 1–10.

Booij, N., Ris, R. C., Holthuijsen, L. H., 1999. A third-generation wave model for coastal regions: 1. Model description and validation. J. Geophys. Res. 104 (C4), 7649.

Bunney, C., 2011. A High Resolution SWAN Model Assessment: North Norfolk to Humber. Tech. Rep. July, MET Office.
URL `www.metoffice.gov.uk`

Caires, S., Sterl, A., Bidlot, J.-R., Graham, N., Swail, V., 2004. Intercomparison of Different Wind-Wave Reanalyses. J. Clim. 17 (10), 1893–1913.

Carbon Trust, AMEC, 2012. Carbon Trust Foreword to UK Wave Resource Study . Tech. Rep. October.

Cavaleri, L., nov 2009. Wave Modeling-Missing the Peaks. J. Phys. Oceanogr. 39 (11), 2757–2778.

Cavaleri, L., Bertotti, L., apr 2006. The improvement of modelled wind and wave fields with increasing resolution. Ocean Eng. 33 (5-6), 553–565.

CEFAS, 2014. CEFAS.
URL `http://www.cefas.defra.gov.uk/home.aspx`

Dee, D. P., Uppala, S. M., Simmons, A. J., Berrisford, P., Poli, P., Kobayashi, S., Andrae, U., Balmaseda, M. A., Balsamo, G., Bauer, P., Bechtold, P., Beljaars, A. C. M., van de Berg, L., Bidlot, J., Bormann, N., Delsol, C., Dragani, R., Fuentes, M., Geer, A. J., Haimberger, L., Healy, S. B., Hersbach, H., Holm, E. V., Isaksen, L., Kallberg, P., Kohler, M., Matricardi,

M., Mcnally, A. P., Monge-Sanz, B. M., Morcrette, J. J., Park, B. K., Peubey, C., de Rosnay, P., Tavolato, C., Thepaut, J. N., Vitart, F., 2011. The ERA-Interim reanalysis: Configuration and performance of the data assimilation system. Q. J. R. Meteorol. Soc. 137 (656), 553–597.

Delft, T., 2014a. SWAN scientific documentation Cycle III version 41.01. Delft University of Technology Faculty of Civil Engineering and Geosciences Environmental Fluid Mechanics Section.

Delft, T., 2014b. SWAN User Manual Cycle III version 41.01.

Dietrich, J., Zijlema, M., Allier, P.-E., Holthuijsen, L., Booij, N., Meixner, J., Proft, J., Dawson, C., Bender, C., Naimaster, A., Smith, J., Westerink, J., nov 2012. Limiters for spectral propagation velocities in SWAN. Ocean Model.

Hasselmann, S., Hasselmann, K., Allender, J., Barnett, T., 1985. Computations and Parameterizations of the Nonlinear Energy Transfer in a Gravity-Wave Specturm. Part II: Parameterizations of the Nonlinear Energy Transfer for Application in Wave Model. Phys. Oceanogr. 15, 1378–1391.

Holthuijsen, L., 2007. Waves in oceanic and coastal waters. Cambridge University Press.

Janssen, P., 2009. The Interaction of Ocean Waves and Wind. Cambridge University Press, Cambridge.

Janssen, P. A., 1991. Quasi-Linear theory of Wind-Wave Generation applied to wave forecasting. J. Phys. Oceanogr. 6, 1631–1642.

Janssen, P. A., mar 2008. Progress in ocean wave forecasting. J. Comput. Phys. 227 (7), 3572–3594.

Komen, G., Cavaleri, L., Donelan, M., Hasselmann, S., Janssen, P., 1994. Dynamics and Modelling of Ocean waves. Cambridge University Press. URL `www.cambridge.org/9780521470476`

Lavidas, G., Venugopal, V., Friedrich, D., 2014. On Investigating Wind - Wave Resource To Enhance Predictability In Offshore Wave Energy Deployments. In: Int. Conf. Offshore Renew. Energy 2014 ASRANET 15th-17th Sept. Glas. 2014. Glasgow.

Richardson, D. S., Bidlot, J., Ferranti, L., Haiden, T., Hewson, T., Janousek, M., Prates, F., Vitart, F., 2013. Evaluation of ECMWF forecasts, including 2012 2013 upgrades. Tech. Rep. November, European Centre for Medium-Range Forecasts (ECMWF).

Ris, R. C., Holthuijsen, L. H., Booij, N., 1999. A third-generation wave model for coastal regions: 2.Verification 104, 7667–7681.

Rogers, W., Hwang, P., Wang, W., 2002. Investigation of Wave Growth and Decay in the SWAN Model : Three Regional-Scale Applications. Phys. Oceanogr., 366–389.

Saha, S., Moorthi, S., Pan, H. L., Wu, X., Wang, J., Nadiga, S., Tripp, P., Kistler, R., Woollen, J., Behringer, D., Liu, H., Stokes, D., Grumbine, R., Gayno, G., Wang, J., Hou, Y. T., Chuang, H. Y., Juang, H. M. H., Sela, J., Iredell, M., Treadon, R., Kleist, D., Van Delst, P., Keyser, D., Derber, J., Ek, M., Meng, J., Wei, H., Yang, R., Lord, S., Van Den Dool, H., Kumar, A., Wang, W., Long, C., Chelliah, M., Xue, Y., Huang, B., Schemm, J. K., Ebisuzaki, W., Lin, R., Xie, P., Chen, M., Zhou, S., Higgins, W., Zou, C. Z., Liu, Q., Chen, Y., Han, Y., Cucurull, L., Reynolds, R. W., Rutledge, G., Goldberg, M., 2010. The NCEP climate forecast system reanalysis. Bull. Am. Meteorol. Soc. 91 (8), 1015–1057.

Sterl, A., Komen, G. J., Cotton, P. D., 1998. Fifteen years of global wave hindcasts using winds from the European Centre for Medium-Range Weather Forecasts reanalysis: Validating the reanalyzed winds and assessing the wave climate. J. Geophys. Res. 103, 5477–5492.

Stopa, J. E., Cheung, K. F., mar 2014. Intercomparison of wind and wave data from the ECMWF Reanalysis Interim and the NCEP Climate Forecast System Reanalysis. Ocean Model. 75, 65–83.

Stopa, J. E., Cheung, K. F., Tolman, H. L., Chawla, A., oct 2013. Patterns and cycles in the Climate Forecast System Reanalysis wind and wave data. Ocean Model. 70, 207–220.

Tolman, H. L., development Group, W. I., 2014. User manual and system documentation of WAVEWATCH III version 4.18. No. 316. Environmental Modeling Center Marine Modeling and Analysis Branch.

Van Der Westhuysen, A. J., Zijlema, M., Battjes, J. a., feb 2007. Nonlinear saturation-based whitecapping dissipation in SWAN for deep and shallow water. Coast. Eng. 54 (2), 151–170.

Venugopal, V., Davey, T., Smith, H., Smith, G., Cavaleri, L., Bertotti, L., John, L., 2010. Equitable testing and evaluation of Marine Energy Extraction Devices of Performance, Cost and Environmental Impact. Deliverable 2.3 Application of Numerical Models. Tech. rep.

WAMDI, G., 1988. The WAM Model-a Third Generation Ocean Wave Prediction Model. Phys. Oceanogr. 18, 1775–1810.

Waveplam, 2009. Methodology for Site Selection (D3.1). Intell. Energy Eur. (November), 1–35.

Zijlema, M., van Vledder, G., Holthuijsen, L., jul 2012. Bottom friction and wind drag for wave models. Coast. Eng. 65, 19–26.